PERGAMON

INTERNATIONAL JOURNAL OF SOLIDS and STRUCTURES

International Journal of Solids and Structures 36 (1999) 3903–3915

Effect of friction on subsurface stresses in sliding line contact of multilayered elastic solids

Abdallah A. Elsharkawy*

Department of Mechanical and Industrial Engineering, College of Engineering and Petroleum, Kuwait University, P.O. Box 5969, Safat 13060, Kuwait

Received 28 May 1997; in revised form 2 June 1998

Abstract

A numerical integral scheme based on Fourier transformation approach is employed to investigate the effect of friction on subsurface stresses arising from the two-dimensional sliding contact of two multilayered elastic solids. The analysis incorporates bonded and unbonded interface boundary conditions between the coating layers. Two line contact problems are presented. The first one is the contact problem between a rigid cylinder and a two-layer half space and the second one is the indentation of a multilayered elastic half-space by a flat rigid punch. The effects of the surface coating on the contact pressure distribution and subsurface stress field are presented and discussed. © 1999 Elsevier Science Ltd. All rights reserved.

Nomenclature

b	half-width of the contact, m
b_H	Hertzian half-width of the contact for nonlayered cylinders $(8w_zR/\pi E')^{1/2}$
E	Modulus of Elasticity, Pa
E'	effective elastic modulus, $2[(1-\nu_a^2)/E_a+(1-\nu_b^2)/E_b]^{-1}$, Pa
$G(\omega, z)$	Fourier transformation function for Airy stress function
N_l	Number of layers
p	pressure, Pa
p_H	maximum Hertzian pressure for nonlayered cylinders $(w_zE'/(2\pi R))^{1/2}$
R	equivalent radius of curvature, $R_aR_b/(R_a+R_b)$, m
R_a	radius of cylinder a, m
R_b	radius of cylinder b, m
t	thickness of layer, m
t_T	total thickness of layers, $\Sigma_{i=1}^{N_l} t_i$

* Fax: 00 965 484 7131; e-mail: abdallah@kuc01.kuniv.edu.kw

0020–7683/99/$ - see front matter
PII: S0020–7683(98)00180–2

u_x displacement in x-direction, m
u_z displacement in z-direction, m
w_z applied normal load, N/m
σ_x normal stress in x-direction, Pa
σ_z normal stress in z-direction, Pa
τ_{xz} shear stress perpendicular to x-direction and in z-direction, Pa
α dimensionless parameter, b/t_T
μ coefficient of friction
ν Poisson's ratio
$\phi(x, z)$ Airy stress function

1. Introduction

A contact problem for multilayered elastic solids is of considerable interest in tribology and other fields of mechanics. Stiff and compliant coatings are used more and more to increase wear resistance of surfaces in contact. For example, in electrical connectors, thin composite layers of gold, nickel and copper alloys are widely used to meet multifunctional requirements.

Either the Fourier transformation approach or the finite element method can be used for computing subsurface stresses in multilayered elastic solids. In terms of actual implementation for practical design the finite element model can be effectively used for arbitrary complex geometry, but the integral formulation is limited to simplified contact configurations. On the other hand, the finite element models require some effort in the pre- and post processing of the data and overall setup of the problem, while the use of the numerical integral model is very straightforward. Thus, depending on the complexity of the application both models may have a notable practical significance. For material selection and preliminary design the Fourier transform approach may be very efficient; for final design development in critical and complex applications, the finite element approach may provide acceptable design solutions with a minimum number of model assumptions and limitations.

The Fourier transformation approach was used by Lemoce (1960), Barovich et al. (1964), Ku et al. (1965), Gupta et al. (1973), and King and O'Sullivan (1987). Lemoce (1960) considered a uniform pressure over the contact zone on a hard layer resting over a relatively soft substrate. Results for stress distributions in the layer and substrate were presented for cases when the layer is either in frictionless contact or bonded to the substrate. Barovich et al. (1964) used an elliptical pressure profile and obtained stress distributions in the materials for various cases when the ratio of the modulus of elasticity of the layer to that of the substrate was in the range 0.25–4. Later Ku et al. (1965) considered surface shear stresses for similar cases. Results were presented for both a uniform and an elliptical shear stress at the layer interface. Subsurface stresses in an elastic half-space with a single layer under actual contact pressures were computed by Gupta et al. (1973) for frictionless contacts and by King and O'Sullivan (1987) for quasi-static sliding contacts. Recently, Mao et al. (1997) developed a numerical technique for evaluating subsurface stresses arising from the multilayered rough sliding contact, considering both normal and tangential loading.

Ihara et al. (1986a, b), Kompovopoulos (1988), Anderson and Collins (1995) computed subsurface stresses in an elastic half space with a single layer by the finite element method. Tian and

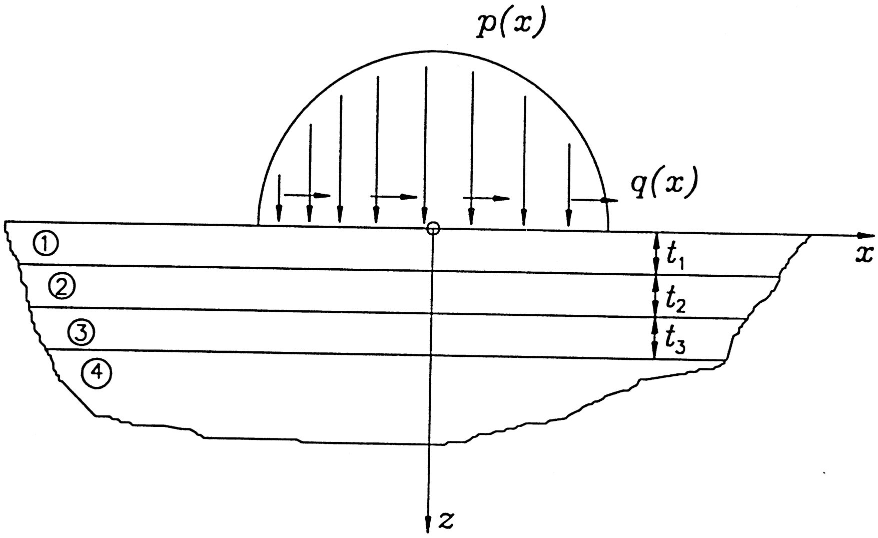

Fig. 1. A multilayered elastic half-space.

Saka (1991) conducted a two-dimensional finite element stress and strain analysis of the sliding contact of a two-layer elastic–plastic half-space. The finite element computer packages such as ABAQUS and ANSYS were used in these studies.

The objective of the present study is to employ a numerical integral scheme based on Fourier transformation approach for evaluating subsurface stresses arising from the two-dimensional sliding contact of two multilayered elastic solids. The analysis incorporates bonded and unbonded interface boundary conditions between the coating layers. Subsurface stresses for two different line contact problems are presented and discussed.

2. Multilayered elastic half-space

Figure 1 shows an elastic half-space coated with a number of thin elastic layers. An arbitrary normal surface traction $p(x)$ and tangential surface traction $q(x)$ are applied on the surface. In sliding contacts, it is usually assumed that the contact pressure distribution is independent of the tangential loading, and the Amonton's law of sliding friction holds, i.e., $q(x) = \mu p(x)$. The general solution for a two-dimensional plane strain problem has been expressed in terms of Fourier integrals (Sneddon, 1951). With reference to the coordinate system shown in Fig. 1, the stresses and the displacements are given by

$$\sigma_x = \frac{\partial^2 \phi}{\partial z^2} = \frac{1}{2\pi}\int_{-\infty}^{\infty} \frac{\mathrm{d}^2 \tilde{G}}{\mathrm{d}z^2} \mathrm{e}^{-i\omega x}\, \mathrm{d}\omega \tag{1}$$

$$\sigma_z = \frac{\partial^2 \phi}{\partial x^2} = -\frac{1}{2\pi}\int_{-\infty}^{\infty} \omega^2 \tilde{G}\, e^{-i\omega x}\, d\omega \tag{2}$$

$$\tau_{xz} = \frac{\partial^2 \phi}{\partial x\, \partial z} = \frac{1}{2\pi}\int_{-\infty}^{\infty} i\omega \frac{d\tilde{G}}{dz} e^{-i\omega x}\, d\omega \tag{3}$$

$$u_x = \frac{1-v^2}{2\pi E}\int_{-\infty}^{\infty}\left[\frac{d^2\tilde{G}}{dz^2} + \left(\frac{v}{1-v}\right)\omega^2\, \tilde{G}\right] i\, e^{-i\omega x}\frac{d\omega}{\omega} \tag{4}$$

$$u_z = \frac{1-v^2}{2\pi E}\int_{-\infty}^{\infty}\left[\frac{d^3\tilde{G}}{dz^3} + \left(\frac{2-v}{1-v}\right)\omega^2\frac{d\tilde{G}}{dz}\right] e^{-i\omega x}\frac{d\omega}{\omega^2} \tag{5}$$

where $\tilde{G}(\omega, z)$ is the Fourier transformation for the Airy stress function $\phi(x, z)$. The transformed function $\tilde{G}(\omega, z)$ can be written for any layer i as

$$\tilde{G}_i(\omega, z_i) = (A_{1,i} + A_{2,i} z_i)\, e^{-|\omega| z_i} + (A_{3,i} + A_{4,i} z_i)\, e^{|\omega| z_i} \tag{6}$$

The coefficients $A_{j,i}(\omega)$, where j = 1, 2, 3, 4 and $i = 1, 2, \ldots, N_1$ (N_1 = number of layers), can be determined by applying the following boundary conditions at the surface and each layer interface with the adjacent layers:

(1) Outside the contact region: $(\sigma_z)_{z=0} = (\tau_{xz})_{z=0} = 0$.
(2) Inside the contact region: $(\sigma_z)_{z=0} = -p(x)$ and $(\tau_{xz})_{z=0} = -q(x) = -\mu p(x)$, where μ is the coefficient of friction between the contacting surfaces.
(3) At a large distance from the contact region: σ_x, σ_z, $\tau_{xz} \to 0$ at $x \to \pm\infty$ and $z \to \infty$.
(4) At the interface between layer i and layer $i+1$:
  (a) If the layers are assumed to be completely bonded, then $(\tau_{xz})_i = (\tau_{xz})_{i+1}$, $(\sigma_z)_i = (\sigma_z)_{i+1}$, $(u_z)_i = (u_z)_{i+1}$, and $(u_x)_i = (u_x)_{i+1}$
  (b) If the layers are assumed to be unbonded, then $(\tau_{xz})_i = (\tau_{xz})_{i+1}$, $(\sigma_z)_i = (\sigma_z)_{i+1}$, $(u_z)_i = (u_z)_{i+1}$ and $(\tau_{xz})_i = \mu_i(\sigma_z)_{i+1}$
  where μ_i is the coefficient of friction at interface between layer i and layer $i+1$.

Details of how the coefficients $A_{j,i}(\omega)$ can be determined are given in Elsharkawy and Hamrock (1993).

3. Subsurface stresses in multilayered elastic solids

Once the contact pressure distribution is determined from dry contact analysis, subsurface stresses can be computed by using the general solution for a two-dimensional plane strain problem in terms of Fourier integrals. The normal stresses σ_x, and σ_z and the shear stress τ_{xz} can be written as follows

$$\sigma_x(X, \zeta) = \frac{\alpha}{\pi}\int_0^{\infty}\left\{\frac{d^2\tilde{G}_{ip}(s, \zeta)}{ds^2} I_1(s, X) + \mu\frac{d^2\tilde{G}_{iq}(s, \zeta)}{ds^2} I_2(s, X)\right\} ds \tag{7}$$

$$\sigma_z(X,\zeta) = -\frac{\alpha}{\pi}\int_0^\infty \{s^2\tilde{G}_{ip}(s,\zeta)I_1(s,X)+\mu s^2\tilde{G}_{iq}(s,\zeta)I_2(s,X)\}\,\mathrm{d}s \tag{8}$$

$$\tau_{xz}(X,\zeta) = \frac{\alpha}{\pi}\int_0^\infty \left\{\frac{\mathrm{d}\tilde{G}_{ip}(s,\zeta)}{\mathrm{d}s}I_2(s,X)-\mu\frac{\mathrm{d}\tilde{G}_{iq}(s,\zeta)}{\mathrm{d}s}I_1(s,X)\right\}\mathrm{d}s \tag{9}$$

where $X = x/b$, $\zeta = z/t_T$, $\alpha = b/t_T$ and

$$I_1(s,X) = \int_{-1}^{1}\cos[\alpha s(X-X')]p(X')\,\mathrm{d}X' \tag{10}$$

$$I_2(s,X) = \int_{-1}^{1}\sin[\alpha s(X-X')]p(X')\,\mathrm{d}X' \tag{11}$$

Subscripts p and q are used in eqns (7)–(9) to denote normal loading and shear loading, respectively. For a uniform pressure approximation in the interval

$$X_j - \frac{\Delta X_j}{2} \leqslant X' \leqslant X_j + \frac{\Delta X_{j+1}}{2}$$

the integrals $I_1(s,X)$ and $I_2(s,X)$ can be written in the following form

$$I_1(s,X) = \sum_{j=1}^{N}\frac{1}{\alpha s}\left\{\sin\left[\alpha s\left(X-X_j+\frac{\Delta X_j}{2}\right)\right]-\sin\left[\alpha s\left(X-X_j-\frac{\Delta X_{j+1}}{2}\right)\right]\right\}p_j \tag{12}$$

$$I_2(s,X) = \sum_{j=1}^{N}\frac{1}{\alpha s}\left\{-\cos\left[\alpha s\left(X-X_j+\frac{\Delta X_j}{2}\right)\right]+\cos\left[\alpha s\left(X-X_j-\frac{\Delta X_{j+1}}{2}\right)\right]\right\}p_j \tag{13}$$

where $\Delta X_j = X_j - X_{j-1}$, $\Delta X_{j+1} = X_{j+1} - X_j$, and N is the number of intervals used to approximate the contact pressure distribution.

For a linear pressure approximation in the interval $X_j \leqslant X' \leqslant X_{j+1}$, the integrals $I_1(s,X)$ and $I_2(s,X)$ can be written in the following form

$$\begin{aligned} I_1(s,X) = {} & \sum_{j=2}^{N-1}\frac{1}{(\alpha s)^2}\frac{1}{X_j-X_{j+1}}\{-\cos[\alpha s(X-X_j)]+\cos[\alpha s(X-X_{j+1})] \\ & +\alpha s(X_j-X_{j+1})\sin[\alpha s(X-X_j)]\}p_j \\ & +\sum_{j=2}^{N-1}\frac{1}{(\alpha s)^2}\frac{1}{X_{j+1}-X_j}\{-\cos[\alpha s(X-X_j)]+\cos[\alpha s(X-X_{j+1})] \\ & +\alpha s(X_j-X_{j+1})\sin[\alpha s(X-X_{j+1})]\}p_{j+1} \end{aligned} \tag{14}$$

$$\begin{aligned} I_2(s,X) = {} & \sum_{j=2}^{N-1}\frac{1}{(\alpha s)^2}\frac{1}{X_j-X_{j+1}}\{-\sin[\alpha s(X-X_j)]+\sin[\alpha s(X-X_{j+1})] \\ & +\alpha s(X_{j+1}-X_j)\cos[\alpha s(X-X_j)]\}p_j \end{aligned}$$

$$+\sum_{j=2}^{N-1}\frac{1}{(\alpha s)^2}\frac{1}{X_{j+1}-X_j}\{-\sin[\alpha s(X-X_j)]+\sin[\alpha s(X-X_{j+1})]$$

$$+\alpha s(X_{j+1}-X_j)\cos[\alpha s(X-X_{j+1})]\}p_{j+1} \tag{15}$$

It was found that integrating eqns (7)–(9) from 0 to s_0 ($s_0 \geqslant 20$) was adequate to give an acceptable accuracy in the results. A semi-open integration formula (Press et al., 1986) was used, since the integrand is singular at $s = 0$.

For the stress field concerned the von Mises equivalent stress σ_{vM} and the maximum shear stress $\tau_{\max}$ are given by

$$\sigma_{vM} = \frac{1}{\sqrt{2}}[(\sigma_x-\sigma_y)^2+(\sigma_y-\sigma_z)^2+(\sigma_z-\sigma_x)^2+6(\tau_{xy}^2+\tau_{yz}^2+\tau_{zx}^2)]^{1/2} \tag{16}$$

$$\tau_{\max} = \left[\left(\frac{\sigma_x-\sigma_z}{2}\right)^2+\tau_{zx}^2\right]^{1/2} \tag{17}$$

where $\tau_{xy} = \tau_{yz} = 0$, $\tau_{xz} = \tau_{zx}$ and $\sigma_y = v(\sigma_x+\sigma_z)$, since plane strain conditions have been assumed. It is well known that yielding occurs when the von Mises equivalent stress σ_{vM} is equal to the yield strength in simple tension σ_Y.

4. Results and discussion

The FORTRAN computer code developed by Elsharkawy and Hamrock (1993) has been modified and extended to calculate subsurface stresses. Some IMSL subroutines such as DLSLRG, DCI, and DSI, were used. Subroutine DLSLRG was used to solve a real general system of linear equations with iterative refinement. Routines DSI and DCI evaluate sine integral and cosine integral, respectively. Various runs were carried out to check the accuracy of the computer program. For the normal contact case with the layers and substrate elastic properties equal, the pressure profile agrees with the Hertzian solution. Furthermore, letting the total thickness of the layers tend to zero and infinity, respectively, the Hertzian solution with appropriate elastic constants was recovered. Gupta and Walowit's (1974) results for the frictionless contact of an elastic solid coated with a single layer and a cylindrical indenter were recovered. King and O'Sullivan (1986) results for the two-dimensional stress analysis of a layer on an elastic half-space under combined normal and sliding line contact were recovered for all the presented cases.

It was found that nonuniform mesh size discretization for the contact zone is more accurate than uniform mesh size discretization at the same number of subintervals. A smaller mesh size was used at the ends of the contact zone because of the steep pressure gradient. The computations were performed on a VAX 9000 computer. Two examples are selected to demonstrate the merits of the present analysis.

4.1. Indentation of a two-layer half-space by a rigid cylinder

Figure 2 shows a rigid cylinder of radius R indenting a two-layer half-space under a normal load per unit width w_z and a tangential load μw_z. The thickness of the top layer and the interlayer are

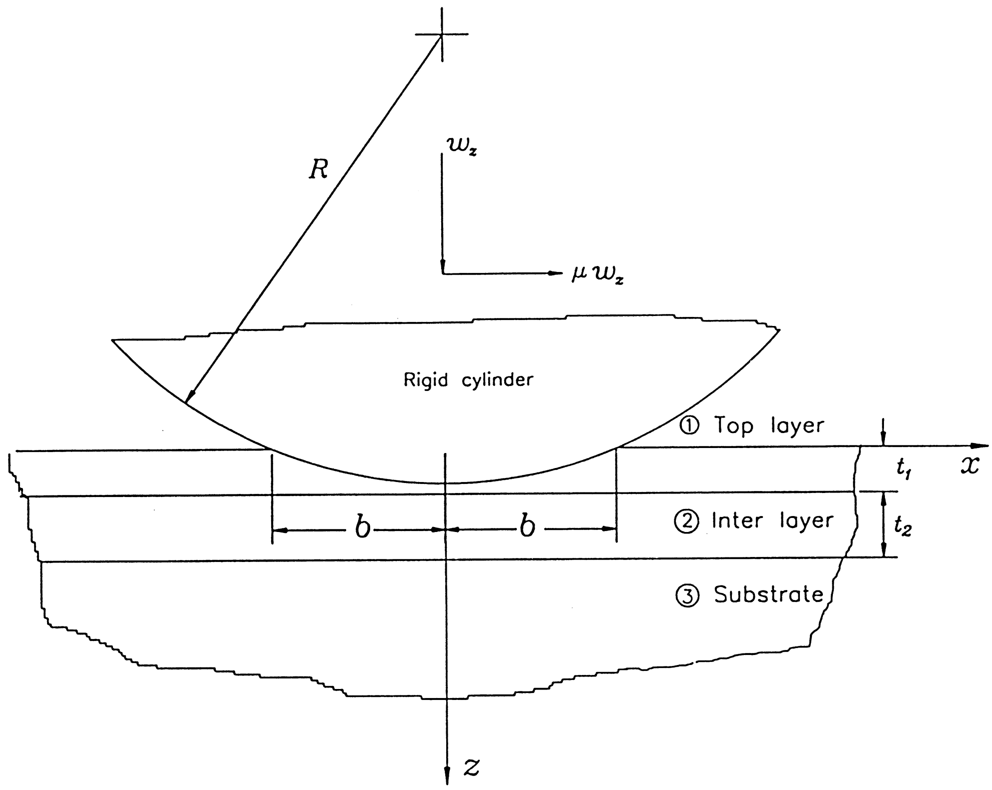

Fig. 2. A two-layer half-space indented by a rigid cylinder.

Table 1
Mechanical properties of coating materials (from Tian and Saka, 1991)

Material	E (GPa)	ν	σ_Y (MPa)
Top layer (Au+0.5%Ni)	79	0.32	298
Interlayer (Ni)	205	0.32	811
Substrate (brass: Cu–35%Zn)	125	0.32	405

t_1 and t_2, respectively. Tian and Saka (1991) solved this case by using the finite element method. Perfect bonding is assumed at the interfaces between layers. Table 1 shows the mechanical properties of the contact materials used in this example. The radius of the rigid cylinder R was taken to be 0.75 mm. The thickness of the top layer and the thickness of the interlayer were chosen at 1.25 and 2.5 μm, respectively. This example represents typical multilayer systems employed in electrical contacts. That is, the top layer is gold, which is hardened with 0.5% nickel, the interlayer is nickel, and the substrate is copper or a copper alloy.

Figure 3 shows von Mises equivalent stress σ_{vM} contours for 5 N/mm normal load for various friction coefficients. For $\mu = 0.1$, the von Mises contours are only slightly different from those of frictionless indentation ($\mu = 0$). As the coefficient of friction increases the location of the maximum value of von Mises equivalent stress moves closer to the surface. Figure 3(c) and Fig. 4 show that at $\mu = 0.3$, the von Mises equivalent stress in the top layer has reached the yield strength, however,

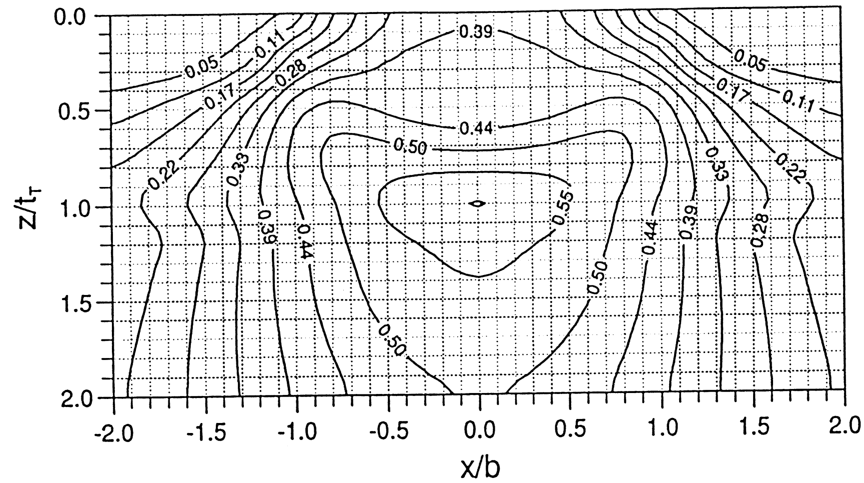

(a) μ = 0.0

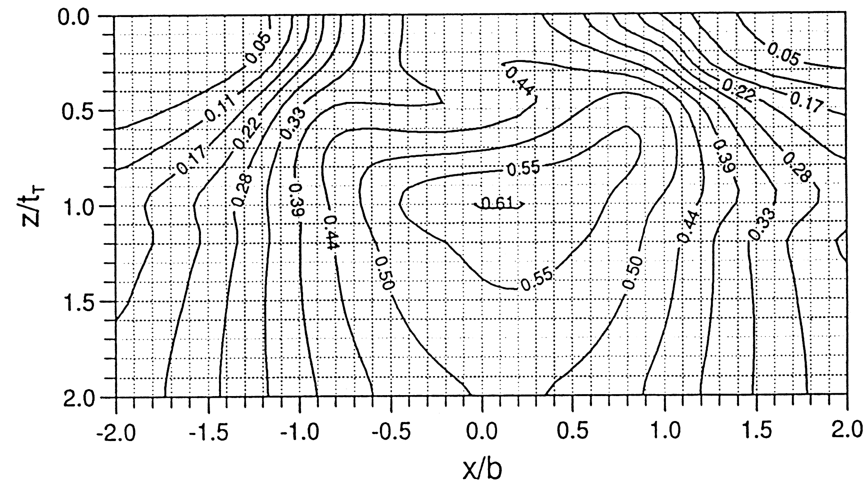

(b) μ = 0.1

Fig. 3. Dimensionless von Mises equivalent stress σ_{vM}/p_H contours for different values of coefficient of friction μ. $t_T = 3.75$ μm, $b_H = 5.855$ μm, and $p_H = 534.62$ MPa: (a) $\mu = 0.0$; (b) $\mu = 0.1$; (c) $\mu = 0.3$; (d) $\mu = 0.5$.

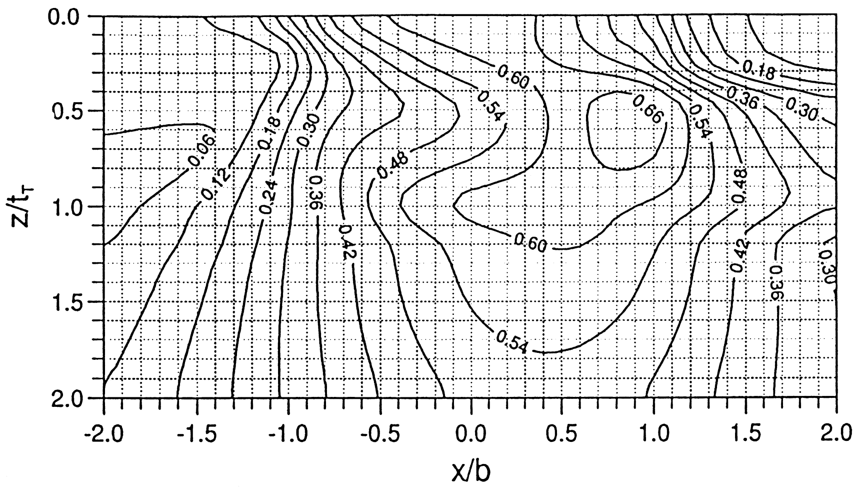

(c) μ = 0.3

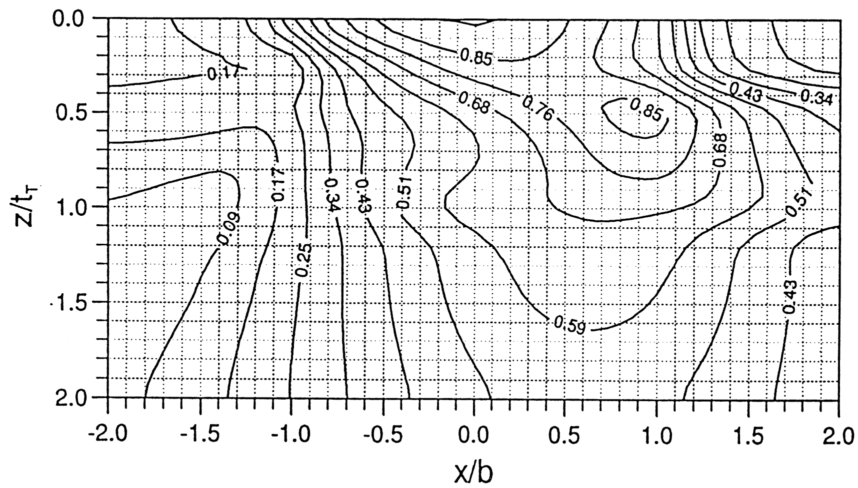

(d) μ = 0.5

Fig. 3—continued.

the maximum von Mises stress occurs inside the interlayer because of its high yield strength (see Table 1). Figure 3(d) shows for $\mu = 0.5$, the von Mises stress contours are further distorted toward the direction of the tangential force. The stresses in the top layer exceeds the yielding strength, while the interlayer and substrate are in the elastic regime.

From the results presented in Figs 3 and 4 we can conclude that subsurface stresses are strongly affected by the friction coefficient. Furthermore, the location of initial yielding strongly depends on the coefficient of friction as well as the applied normal load. The results presented in Figs 3 and

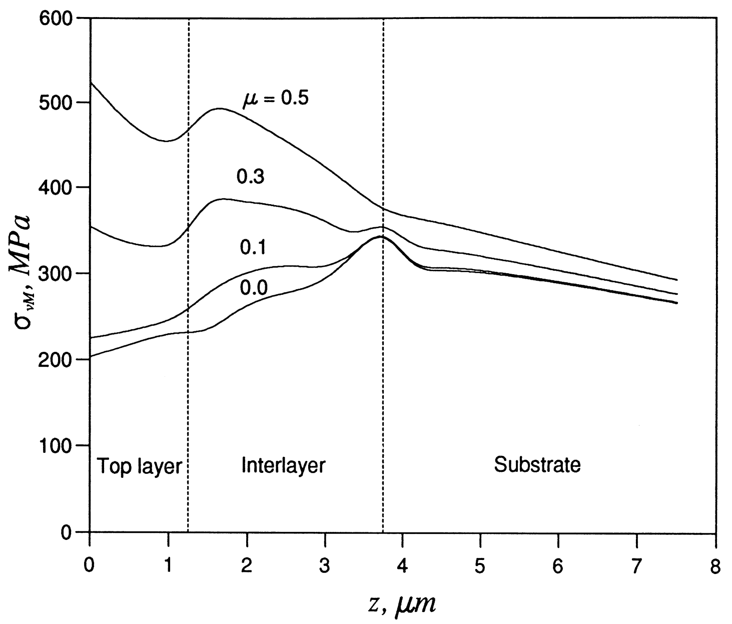

Fig. 4. Effect of coefficient of friction μ on the maximum value of von Mises equivalent stress σ_{vM}.

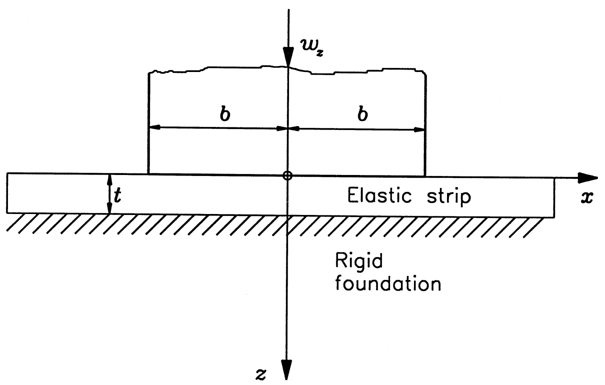

Fig. 5. An elastic strip of finite thickness resting on rigid foundation and indented by a flat rigid punch.

4 are in a good agreement with the results presented in Tian and Saka (1991) for the same example. Note that Tian and Saka (1991) used the multi-purpose finite element program (ABAQUS) in their analysis.

4.2. *Indentation of an elastic strip by a rigid punch*

Figure 5 shows an elastic strip of finite thickness resting on a rigid foundation and indented by a flat rigid punch. The interface between the strip and the foundation can be bonded or unbonded.

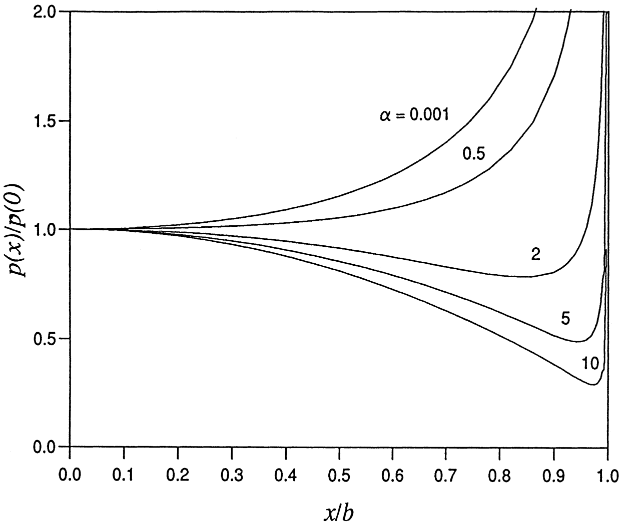

Fig. 6. Influence of α on dimensionless pressure $p(x)/p(0)$ distribution for a flat punch when $v = 0.5$ and the strip is bonded with the foundation.

This example was solved by Jaffar and Savage (1988) by solving the integral equation numerically by a method proposed by Gladwell (1976). In this method the unknown pressure distribution is expanded in terms of Chebyshev polynomials of the first kind. Jaffar and Savage (1988) showed that Gladwell's method is quite general in the sense that it is easily applied to any punch profile of a polynomial of degree n and give results in the range $0 \leqslant \alpha \leqslant 10$ for Poisson's ratio $0 \leqslant v \leqslant 0.5$. For the analysis presented in this paper, the substrate can be coated by any number of layers and the effects of sliding friction can be studied.

Figure 6 shows the effect of α ($\alpha = b/t$) on the pressure distribution while the coefficient of friction μ and the Poisson's ratio v were held fixed at 0.0 and 0.5, respectively, and the strip is perfectly bonded into the rigid foundation. As α increases (i.e. the strip becomes thinner) the pressure dip increases. Figure 7 is similar to Fig. 6 but for unbonded strip. In the case of unbonded strip the pressure dips are much less pronounced. The results presented in Figs 6 and 7 are in a good agreement with those of Jaffar and Savage (1988). Qualitatively, this phenomenon of a pressure dip occurred when α is large (thin strip) because pressure falls with distance from the center of the contact (a one-dimensional effect) and subsequently rises to infinity at the end of the contact (see mathematical interpretation in Jaffar and Savage, 1988).

Pressure distributions over the contact zone for $\alpha = 2$ and $v = 0.5$ and different values of the coefficient of friction μ are shown in Fig. 8. The effect of friction is to increase the pressure in the direction of the tangential force. It is apparent that the influence of frictional traction upon normal pressure for this case is significant.

5. Conclusions

A numerical integral scheme based on Fourier transformation approach for evaluating sub-surface stresses arising from the two-dimensional sliding contact of two multilayered elastic solids

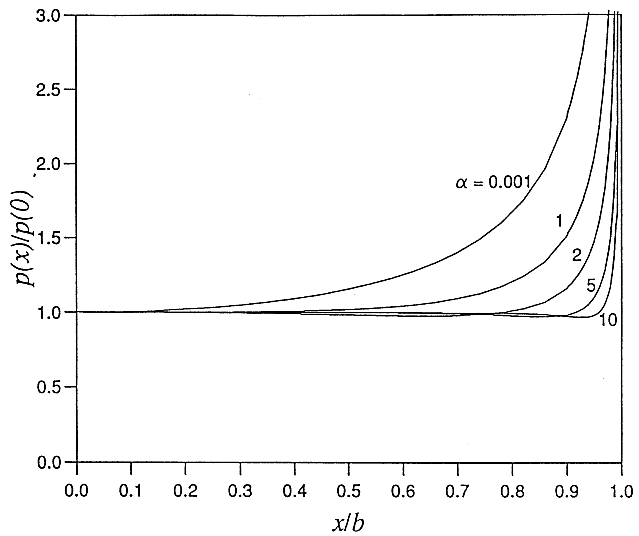

Fig. 7. Influence of α on dimensionless pressure $p(x)/p(0)$ distribution for a flat punch when $v = 0.5$ and the strip is unbonded with the foundation.

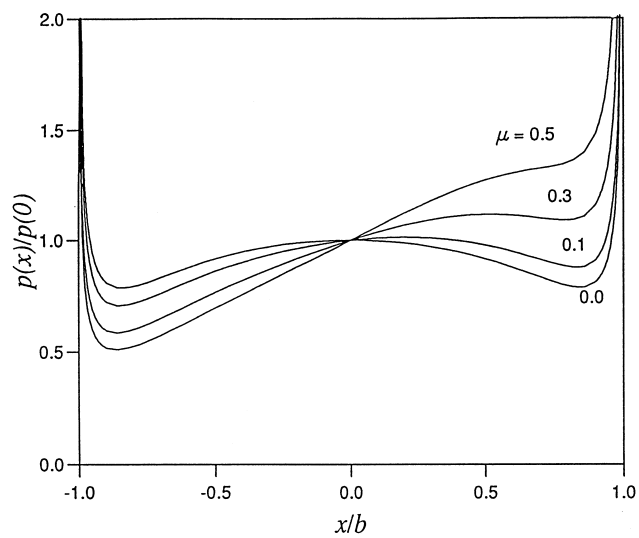

Fig. 8. Dimensionless pressure $p(x)/p(0)$ distributions for different values of coefficient of friction μ when $\alpha = 2$ and $v = 0.5$.

has been presented. The analysis incorporates bonded and unbonded interface boundary conditions between the coating layers. Two line contact problems are presented. The first one is the contact problem between a rigid cylinder and a two-layer half space and the second one is the indentation of a two layer half-space by a flat rigid punch. The following conclusions can be drawn from the results presented in this paper:

(1) Subsurface stresses are strongly affected by the friction coefficient. The location of initial yielding strongly depends on the coefficient of friction as well as the applied normal load.
(2) The interface boundary condition between the coating layers has a significant effect on the contact pressure distribution.
(3) The Fourier transform approach is very efficient and can be used for material selection and preliminary design stages.

References

Anderson, I.A., Collins, I.F., 1995. Plane strain stress distributions in discrete and blended coated solids under normal and sliding contact. Wear 185, 23–33.

Barovich, D., Kingsley, S.C., Ku, T.C., 1964. Stresses on a thin strip or slab with different elastic properties from that of the substrate due to elliptically distributed load. International Journal of Engineering Sciences 2, 253–267.

Elsharkawy, A.A., Hamock, B.J., 1993. A numerical solution for dry sliding line contact of multilayered elastic solids. ASME, Journal of Tribology, 115 (2), 237–245.

Gladwell, G.M.L., 1976. On some unbonded problems in plane elasticity theory. ASME, Journal of Applied Mechanics 43, 263–267.

Gupta, P.K., Walowit, J.A., 1974. Contact stresses between a cylinder and a layered elastic solid. ASME, Journal of Lubrication Technology 96, 250–257.

Gupta, P.K., Walowit, J.A., Finkin, E.F., 1973. Stress distributions in plane strain layered elastic solids subjected to arbitrary boundary loading. Trans. ASME, Journal of Lubrication Technology 95 (Ser. F, No. 4), 427–433.

Ihara, T., Shaw, M.G., Bhushan, B., 1986a. A finite element analysis of contact stress and strain in an elastic film on a rigid substrate—Part I: Zero friction. Trans. ASME, Journal of Tribology, 108 (4), 527–533.

Ihara, T., Shaw, M.G., Bhushan, B., 1986b. A finite element analysis of contact stress and strain in an elastic film on a rigid substrate—Part II: With friction. Trans. ASME, Journal of Tribology 108 (4), 534–539.

Jaffar, M.J., Savage, M.D., 1988. On the numerical solution of line contact problems involving bonded and unbonded strips. Journal of Strain Analysis 23 (2), 67–77.

King, R.B., O'Sullivan, T.C., 1987. Sliding stresses in a two-dimensional layered elastic half-space. International Journal of Solids and Structures, 23 (5), 581–597.

Komovopoulus, K., 1988. Finite element analysis of a layered elastic solid in normal contact with a rigid substrate. ASME, Journal of Tribology, 110 (3), 477–485.

Ku, T.C., Kingsley, S.C., Ramsey, H., 1965. Stresses in a thin slab with different elastic properties from that of the substrate due to distributed normal and shearing forces on the surface of the slab. International Journal of Engineering Sciences 3, 93–107.

Lemcoe, M.M., 1960. Stresses in layered elastic solids. Proceedings, ASCE, EM4, p. 1.

Mao, K., Bell, T., Sun, Y., 1997. Effect of sliding friction on contact stresses for multilayered elastic bodies with rough surfaces. Trans. ASME, Journal of Tribology 119, 476–480.

Press, W.H., Flannery, B.P., Teukolsky, S.A., Vetterling, W.T., 1986. Numerical Recipes, The Art of Scientific Computing. Cambridge University Press, pp. 108–110.

Sneddon, I.N., 1951. Fourier Transformation. McGraw-Hill.

Tian, H., Saka, N., 1991. Finite element analysis of an elastic–plastic two-layer half-space: sliding contact. Wear, 148, 262–285.